Depletion interaction in a quasi-two-dimensional binary colloid mixture: Monte Carlo simulations

Alice Sheu and Stuart A. Rice
Department of Chemistry and The James Franck Institute, The University of Chicago, Chicago, Illinois 60615, USA
(Received 1 October 2004; published 25 July 2005)

We report the results of extensive calculations of the depletion interaction between the large hard spheres in a quasi-two-dimensional (q2D) binary mixture of large and small hard spheres. Two definitions of the depletion interaction have been examined, and the dependencies of both on the large and small sphere densities, and the confining wall separation have been explored. The results of the simulations show that the depletion interaction is enhanced relative to its magnitude in a three-dimensional binary mixture with the same density, composition and sphere diameter ratio and that it has a complex dependence on the large sphere-large sphere separation. There are qualitative differences between the properties of q2D and mathematical 2D systems that are relevant to the interpretation of experimental data.

DOI: 10.1103/PhysRevE.72.011407 PACS number(s): 82.70.Dd, 61.20.Ja, 61.20.Lc, 66.30.−h

I. INTRODUCTION

The work reported in this paper was undertaken to provide a detailed molecular interpretation of the enhancement of the depletion interaction in a quasi-two-dimensional (q2D) binary colloid mixture, relative to that in the equivalent three-dimensional (3D) system, that has been observed in recent experiments [1]. There are good reasons to expect that the depletion interaction in a q2D binary colloid system will be somewhat different from that in a 3D system with the same composition and sphere diameter ratio. For example, the extant analyses of the character of the wall sphere interaction in a binary hard sphere mixture show that there is an enhancement of the wall-large sphere effective interaction that is generated by the small spheres in the mixture [2,3]. The origin of this enhancement is the increase in volume available to the centers of the small (S) spheres when the wall and the center of a large (L) sphere are separated by less than the sum of the large and small sphere diameters (σ_L and σ_S, respectively). Since, in a q2D system a pair of colloid particles is always close to the walls [4,5], it is to be expected that the depletion interaction between them will be altered from that in 3D. However, almost all of the existing theoretical descriptions of the depletion interaction between spheres restrict attention to the properties of unconfined 3D binary mixtures of large and small hard spheres. The Asakura–Oosawa model of such mixtures, which assumes that the small particles can be treated as an ideal gas, predicts that the depletion interaction is purely attractive in the particle separation range, with magnitude proportional to the small particle density [6,7]. Later theoretical analyses have removed the restrictions imposed in the Asakura–Oosawa model; they find, in general, that the depletion interaction is monotone attractive when the small sphere density is small, but that it becomes structured when the small sphere density is increased [8–11].

In the q2D systems of interest to us the large and small colloid particles are confined between plates that are separated by less than $\sigma_L+\sigma_S$, so that the small colloid particles cannot pass "over" or "under" the large colloid particles, although they can pass "around" them. Because the centers of the large spheres can lie somewhat above and below the center plane of the q2D container, and because the small sphere centers can move in a constrained 3D volume, the systems we consider are different from the conventional 2D model mixture of large and small disks, the centers of all of which are constrained to move in one plane. An extensive study of the depletion interaction in a binary hard disc mixture has been reported by Castaneda-Priego *et al.* [12], We compare our findings with theirs in Sec. IV. We argue that the systems we consider are closer to the experimental realizations of q2D binary mixtures than are 2D systems since the experimental studies concern large colloid motion in the presence of smaller colloids in a cell with wall separation that is both slightly greater than the diameter of the large colloid particle and a multiple of the diameter of the small colloid particle that is greater than the ratio of particle diameters. We have carried out Monte Carlo simulations of q2D binary hard sphere mixtures for a range of plate separations defining the q2D sample cell and for a range of large and small sphere densities. The results of these simulations provide a useful data set against which analyses of diverse properties of q2D binary hard sphere mixtures can be tested. The particular test of interest to us is the magnitude and form of the depletion interaction between a pair of large hard spheres. As already indicated, it is expected that the volume excluded to the center of a small particle by a pair of large particles depends on the proximity of the particles to the walls of the q2D container, and the large sphere–large sphere depletion interaction that is generated by the small spheres is thereby enhanced. The results of our simulations show this enhancement, but they fail to account for the magnitude of the observed enhancement of the depletion interaction in the q2D system [1]. One possible explanation for this failure, the existence of distributions of large and small sphere diameters in the experimental system, is described in another paper [13]; it too fails to account for the observed enhancement of the depletion interaction. Our results, and those of other calculations [13] suggest that the real experimental situation is not completely modeled by the simulations. One such omis-

sion, neglect of the character of the interface between the hydrophobic sample cell walls and the water suspension of colloid particles that exists in the experimental system, is likely more important than previously believed. We suggest that an interplay between neglected capillary forces and confinement forces leads to enhancement of the q2D depletion interaction beyond that calculated in this paper.

II. SIMULATION DETAILS

We have calculated, by Monte Carlo simulations, the properties of a binary hard sphere mixture constrained to occupy the space between two flat smooth hard plates. To create a q2D assembly of particles the separation of the plates, H, was required to satisfy the constraint $H<2\sigma_L$; the range of H actually studied was $1.1\sigma_L \leqslant H \leqslant 1.8\sigma_L$. All of our calculations were carried out in the canonical ensemble representation, with N_L large hard spheres, N_S small hard spheres and with a small sphere to large sphere diameter ratio of $q \equiv \sigma_S/\sigma_L = 0.30$. Periodic boundary conditions were applied to the simulation cell in the x and y directions. By virtue of the constraint on H, in this simulation cell the motions of the large sphere centers are quasi-two-dimensional, hence we characterize the large hard sphere subsystem with the density $\rho_L = N_L/A$, with A the area of the simulation cell. As to the motions of the small sphere centers, when $1.1\sigma_L \leqslant H \leqslant 1.3\sigma_L$ the small spheres cannot pass "over" or "under" the large spheres, although they can pass "around" them, and when $1.3\sigma_L \leqslant H \leqslant 1.8\sigma_L$ the small spheres can move in three dimensions. Simulations have been carried out for each value of H considered, as a function of ρ_L, and the small sphere packing fraction, $\eta_S \equiv \sigma_S^3 N_S/6V$, with V the volume of the simulation cell. Variation of the large sphere density was achieved by changing the simulation cell dimensions and variation of the small sphere packing fraction by changing N_S. All of our results are reported in reduced units defined by setting the large sphere diameter $\sigma_L = 1$.

We have chosen to carry out simulations for liquid densities close to but below the liquid–solid phase transition; at all densities studied the binary hard sphere mixture is isotropic in the xy plane. The density distribution therefore depends only on the distance from the wall and we collect $\rho(z)$ along the perpendicular to the wall. We notate the large sphere pair correlation function as $g_{LL}(\mathbf{r_1}, \mathbf{r_2}, z_1, z_2) \equiv g_2(|\mathbf{r_1} - \mathbf{r_2}|, z_1, z_2)$ where $\mathbf{R_i} = (x_i, y_i, z_i)$ is the location of the center of particle i. In order to display the dependence of g_2 on $|\mathbf{r_1} - \mathbf{r_2}| = r_{12}$ we take thin parallel slices of width $2\delta z = 0.1$ at the center of the cell $(z_1 = z_2 = \pm \delta z)$ and close to the walls $[z_1 = z_2 = \pm(h - \delta z), h = (H - \sigma_L)/2]$ and collect pair correlation functions within. The thicknesses of the slices are fixed at $2\delta z = 0.1$, regardless of the value of H; hence the system is viewed as a single slice when $H = 1.1$ and the three slices are immediately adjacent to each other when $H = 1.3$.

III. SIMULATION RESULTS

A. Density distribution perpendicular to the wall

The normalized density distributions of the large spheres in the binary mixture along the z axis, $\rho_L(z)$, are displayed in Fig. 1(b) for several values of H for fixed values of $\rho_L = 0.8$, $\eta_S = 0.028$, and $q = 0.3$. The values of H for which data are displayed, namely 1.1, 1.3, 1.5, and 1.8 (in units of σ_L), correspond to plate separations of 3.3, 4.3, 5.0, and 6.0 σ_S. When $H = 1.8\sigma_L$, the density of large spheres in the center of the q2D cell is small (of order one-fifth the density at the wall). The exclusion of the large spheres from the center of the cell is greater than in the corresponding one component large sphere system [see Fig. 1(a)], consistent with studies of the influence of small spheres on the single wall-large sphere effective interaction [2]. The distribution of large sphere centers parallel to the wall exhibits a tendency towards buckling similar to that found in simulations of the solid phase [5,14]. This buckling is more prominant at smaller values of H when small spheres are present.

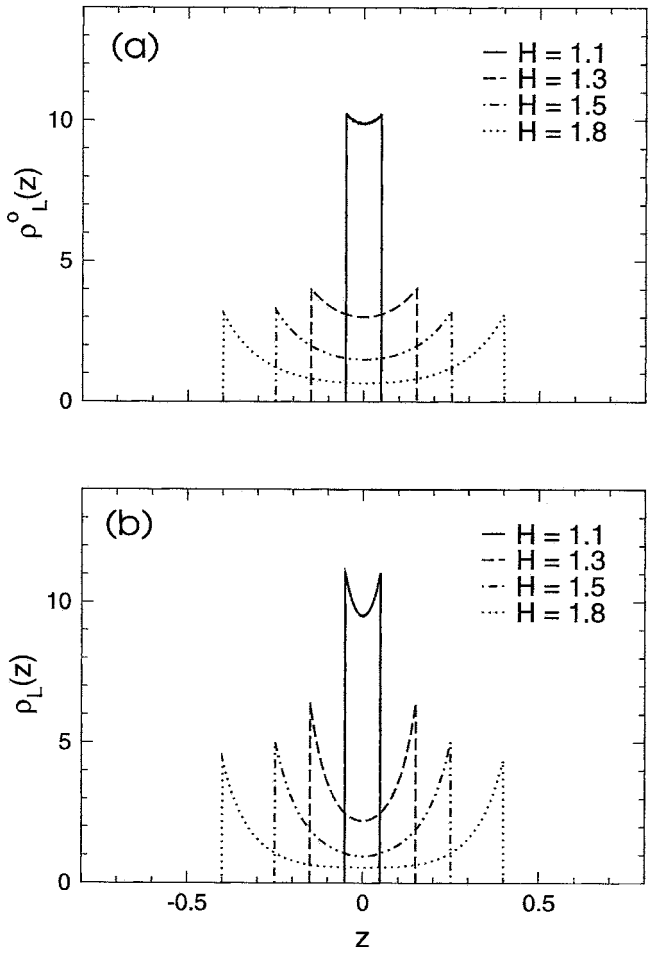

FIG. 1. (a) $\rho_L(z)$ in the absence and (b) in the presence of small spheres ($\eta_S = 0.028$) as a function of H when $\rho_L = 0.8$ and $q = 0.3$.

Figure 2 displays the small sphere distribution function $\rho_S(z)$ for the same parameter set as in Fig. 1(b). The results clearly show that the density of small spheres around the large spheres is not uniform; the contact density at the wall is very high and the density distribution between the walls is almost flat. A necessary implication of this result is that the Asukura–Oosawa model is not applicable in the q2D systems we have studied. The Asukura–Oosawa assumption that the small spheres form an ideal gas [6,7] implies that the distribution of small spheres will be uniform along the z axis,

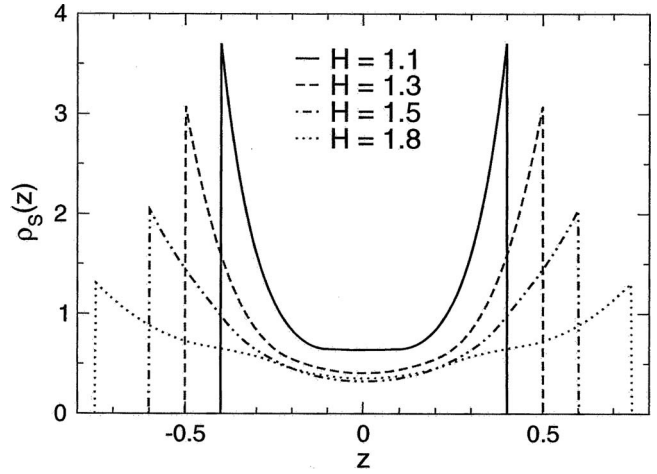

FIG. 2. $\rho_S(z)$ as a function of H in a q2D binary hard sphere mixture with $\rho_L=0.8$, $q=0.3$, and $\eta_S=0.028$.

independent of the presence or absence of large spheres [15]; the obvious source of the failure is the neglect of excluded volume interactions between the small hard spheres. Comparison of $\rho_S(z)$ in the binary hard sphere mixture with the equivalent distribution function in a one-component small sphere system as a function of H [4] shows that, as H increases, $\rho_S(z)$ in the presence of large spheres is more spread out than in their absence, and that the ordering of the small spheres parallel to the cell walls is almost destroyed by the presence of the large spheres.

B. Pair correlation functions

The large sphere pair correlation function depends on z_1 and z_2 as well as the separation of the particles. We note that for the large spheres in our q2D system $|z_1,z_2| \leqslant (H-\sigma_L)/2 = h$. Figure 3 shows the dependence on H of the large sphere pair correlation functions in (a) center and (b) wall slices of width $2\delta z=0.1\sigma_L$. Note that the positional correlation weakens as H increases. The weakening of the positional correlation in the slice adjacent to the wall is rather extreme when $H=1.8$, which appears to be anti-intuitive given the large particle density in that layer. However, the slices adjacent to the wall are not independent of each other since we are working at wall separations smaller than $2\sigma_L$. The slices are divided according to the positions of the *center* of the spheres, but spheres in different slices actually overlap in the z direction due to the nonzero particle size. The positions of the large spheres in the slice adjacent to one wall, therefore, tend to be anticorrelated with the positions of the large spheres adjacent to the other wall, because of the hard sphere-hard sphere interactions between them, which leads to destruction of positional correlation within the individual slices.

It is important to note that in this series of calculations it is the two-dimensional number density ρ_L that is kept constant as H increases; calculations in which the 3D density of the large spheres is kept constant are not feasible, as one then encounters a phase transition going from 3D to q2D [14].

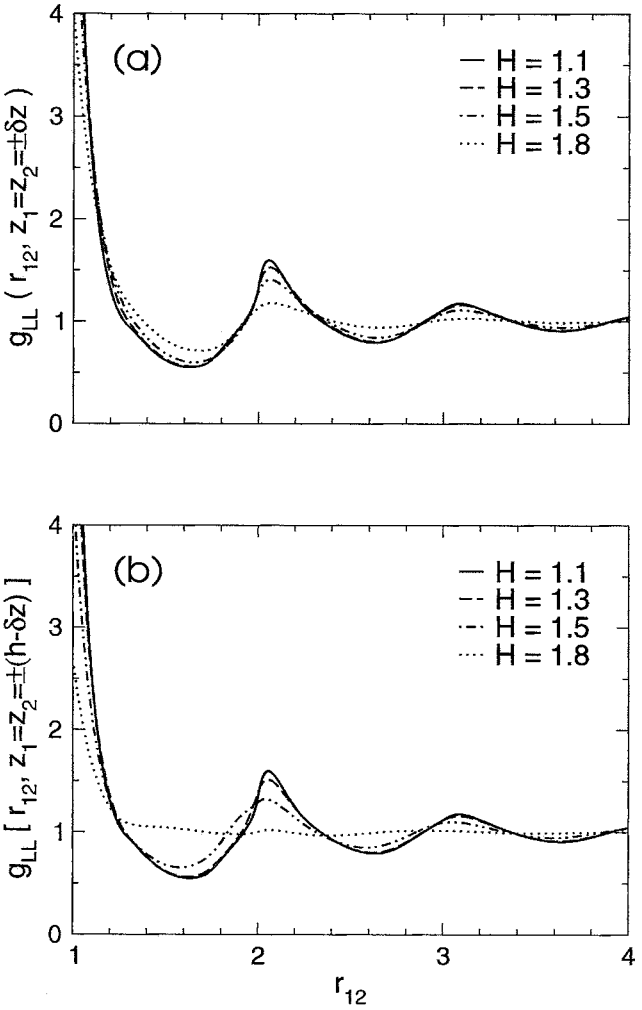

FIG. 3. Large sphere pair correlation functions (a) in the center and (b) at the wall of the q2D cell as a function of H when $\rho_L=0.8$, $q=0.3$, and $\eta_S=0.028$.

The influence of variation of the small sphere density (hence variation of the depletion interaction) on the large sphere pair correlation function is shown in Fig. 4 for the fixed wall separation $H=1.1$. At this wall separation the center and wall slices coincide with each other and we view the system as a single slice. The influence of the depletion interaction is most pronounced at the first peak of the correlation function, changing the shape of the falloff from the peak as the particle separation increases. The presence of small spheres in the hard sphere mixture also slightly increases the amplitude of the second peak and changes the shape of its falloff as the particle separation increases. There is very little influence of the small sphere concentration on the third peak except for a slight phase shift. These changes are consistent with the view that the small spheres alter the ordering of the large spheres in the binary hard sphere mixture.

C. Depletion potential

The depletion interaction is designed to provide a quantitative measure of the influence of one component in a binary mixture on the structure of the other component when the

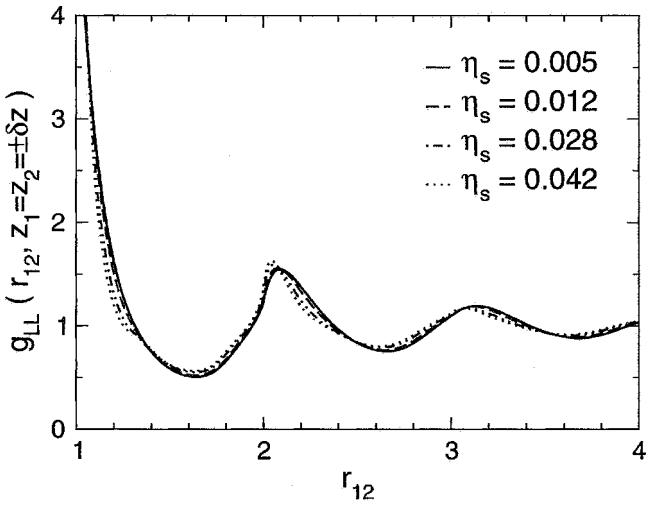

FIG. 4. Large sphere pair correlation functions of the q2D cell as a function of η_S: $H=1.1$, $\rho_L=0.8$, and $q=0.3$.

latter is considered to be a pseudo-one-component system. That quantitative measure can take different forms depending on the way the difference in structure is viewed. For example, if interest is focused solely on how the pair correlation function of a hard sphere liquid is influenced by addition of smaller hard spheres, one possible definition of the depletion interaction is the difference between the potentials of mean force for the large spheres with the same density in the systems with and without the small spheres:

$$\Delta\omega = \omega^{\mathrm{mix}} - \omega^0 = -k_BT \ln g_{LL}^{\mathrm{mix}} + k_BT \ln g_{LL}^0. \quad (3.1)$$

In Eq. (3.1), ω^0 and g_{LL}^0 are the potential of mean force and the pair correlation function in the pure large sphere system with the same large sphere density as in the binary mixture. This definition is applicable to fluid mixtures with arbitrary density and composition. It has the advantage of separating directly the structure that is associated with the packing of the large spheres when present alone from that induced by the addition of small spheres. As defined, $\Delta\omega$ is the excess work needed to bring a pair of large spheres from infinite separation to separation in the presence of a specified density of small spheres, relative to carrying out the same process in the absence of small spheres.

A different measure of the depletion interaction is commonly used in the literature on this subject, namely the difference between the effective pair interaction between the large spheres in the presence and absence of the small spheres. Using the same notation as in Eq. (3.1),

$$\Delta u_{\mathrm{eff}} = u_{\mathrm{eff}}^{\mathrm{mix}} - u_{LL}^0. \quad (3.2)$$

From the point of view of an experimenter, $\Delta\omega$ can be calculated directly from the measured large particle pair correlation functions of the mixture and the corresponding pure liquid. However, to calculate Δu_{eff} from the same experimental data the pair correlation function must be inverted using, say, an integral equation representation, or a reverse Monte Carlo simulation must be carried out, all under the assumption that the effective interaction between the large spheres is pair additive. From the point of view of a theorist, the notion behind the definition (3.2) is that integration over the coordinates of the second component spheres maps the mixture onto a pseudo-one-component system in which the pair interaction is $u_{\mathrm{eff}}^{\mathrm{mix}}$. The most widely accepted definition of the depletion interaction is based on the McMillan–Mayer theory of solutions [16], and it deals with the case of a pair of large particles embedded in a sea of small particles held at a specified chemical potential. That definition is not the most useful when the system under examination has a high density of large particles. In this paper we compare the descriptions of the q2D depletion interaction defined in Eqs. (3.1) and (3.2). To calculate Δu_{eff} we make use of the inverse Monte Carlo technique described in [17], with the iterative algorithm described by Frydel and Rice [13].

For an unconstrained (3D) pure hard sphere system, u_{LL}^0 is zero for $r_{12}>1$. We are interested in how the structure of the large particles in a q2D system in planes parallel to the confining walls varies along the line perpendicular to the confining walls. In the q2D systems that we are interested in, $H<1.8$, so the particles in a particular z-slice overlap the plane of centers of the particles in adjacent z-slices. Then the effective potential that determines the structure in one slice is not u_{LL}^0, but rather one that includes the influence of the particles outside of the slice. It is therefore more appropriate to rewrite Eq. (3.2) to apply to each slice (i) separately:

$$\Delta u_{\mathrm{eff}}(i) = u_{\mathrm{eff}}^{\mathrm{mix}}(i) - u_{\mathrm{eff}}^0(i). \quad (3.3)$$

Of course, Eq. (3.3) reduces to (3.2) for each slice in the limit $\rho_L \to 0$. However, when $\rho_L \neq 0$ the effective potential that generates the pair correlation function in slice i is a density dependent free energy that differs considerably from the bare hard core interaction.

Figure 5 shows the effective pair potential for pure hard spheres, $u_{\mathrm{eff}}^0(i)$, in the q2D simulation at the center of the cell and at the walls of the cell. There are substantial differences between $u_{\mathrm{eff}}^0(i)$ and u_{LL}^0. When $H=1.1$, the entire q2D system is treated as a single slice since each of the slices is $0.1\sigma_L$ thick. In that case $u_{\mathrm{eff}}^0(i)$ is sensibly indistinguishable from u_{LL}^0, i.e., it is zero for $r_{12}>1$. When $H=1.3$, the density of large spheres adjacent to a wall is greater than that in the center, so the different z slices have different densities, and the spheres in each slice overlap the plane of centers of the adjacent slices. The excluded volume constraints generated by those overlaps are represented in $u_{\mathrm{eff}}^0(i)$ by an oscillatory variation with increasing r_{12} with period equal to the large sphere diameter; the maximum negative amplitude of the variation of $u_{\mathrm{eff}}^0(i)$ occurs when $r_{12}=1$ and is about $-1.4k_BT$, while the maximum positive amplitude occurs when r_{12} is about 1.5 and is about $0.55k_BT$. The differences between $u_{\mathrm{eff}}^0(i)$ and u_{LL}^0 are maximal for the intermediate cell thicknesses $H=1.3$ and 1.5. When $H=1.5$ the density at the wall is smaller than when $H=1.3$, but the difference is small enough that $u_{\mathrm{eff}}^0(i)$ is only slightly different from the case when $H=1.3$. When $H=1.8$ $u_{\mathrm{eff}}^0(i)$ is sensibly zero for $r_{12}>1.3$ and the attractive amplitude at $r_{12}=1$ is considerably decreased relative to its values when $H=1.3$ and 1.5. The direction of the shift in the position of the peak value of $u_{\mathrm{eff}}^0(i)$ with H, to

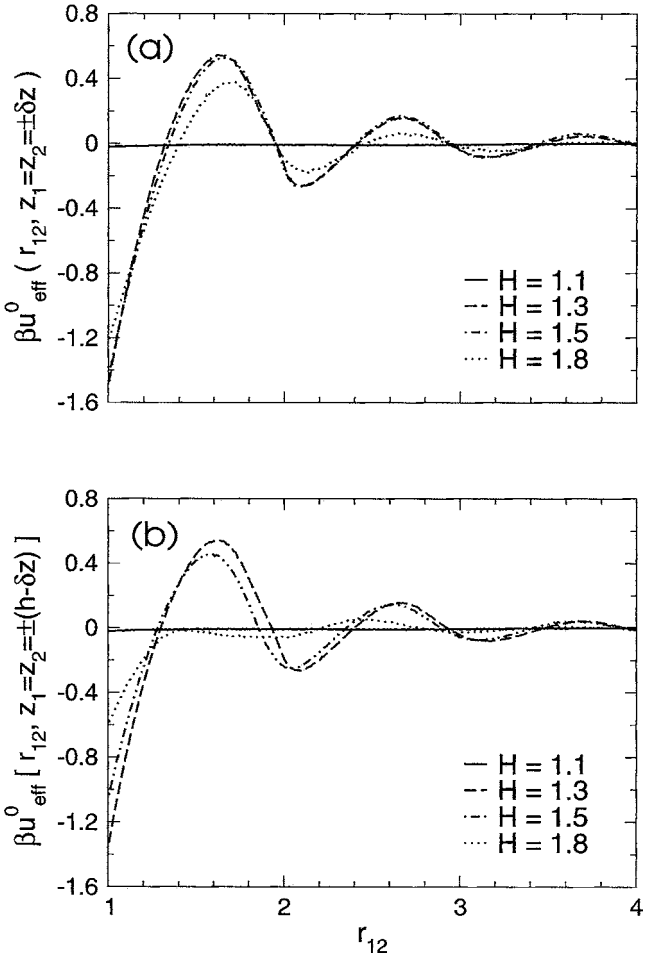

FIG. 5. Effective pair potentials of pure hard sphere systems (a) at the center and (b) at the wall as a function of H.

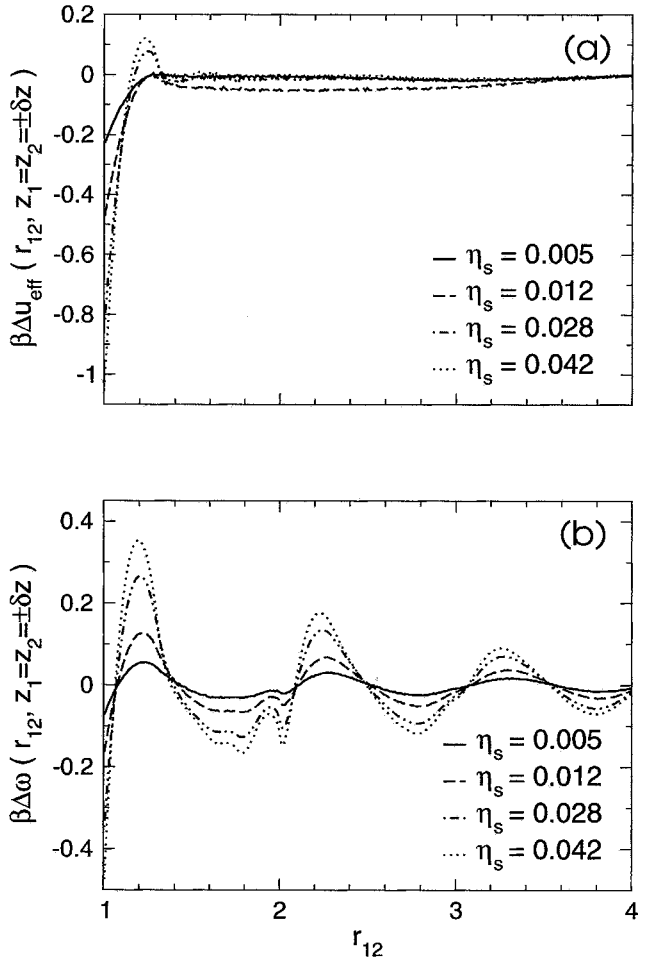

FIG. 6. (a) $\Delta\omega$ and (b) Δu_{eff} as a function of η_S when $H=1.1$, $\rho_L=0.8$, and $q=0.3$.

smaller r_{12}, arises because the sphere closest to a chosen sphere is more likely to be in the other wall slice and the penetration of the two slices has the consequence that the distance between adjacent spheres become shorter when projected onto the other wall slice.

The dependence of Δu_{eff} on the concentration of the small spheres is shown in Fig. 6(a) for the case $\rho_L=0.8$, $q=0.3$, and $H=1.1$. Clearly, Δu_{eff} is almost purely attractive when η_S is small, but a repulsive component grows in rapidly as η_S increases; the barrier is located at $r_{12}=1+(\sigma_S/\sigma_L)$. When $\eta_S=0.042$ the repulsive barrier has a height of about 0.1 k_BT and the attractive well a depth of about k_BT.

The dependence of $\Delta\omega$ on the concentration of the small spheres is shown in Fig. 6(b) for the case $\rho_L=0.8$, $q=0.3$, and $H=1.1$. The r_{12} dependence of $\Delta\omega$ is somewhat more complex than that of Δu_{eff}. The large oscillations in $\Delta\omega$ indicate that as the concentration of small spheres increases there is a greater and greater tendency to form concentric shells of large and small spheres. Thus, as η_S increases the density of pairs of large spheres with separations slightly less than $r_{12}=1+(\sigma_S/\sigma_L)$, $2+(\sigma_S/\sigma_L)$, and $3+(\sigma_S/\sigma_L)$ decreases. There is also a weaker region of exclusion near $r_{12}=2$, and $\Delta\omega$ is attractive in the region $r_{12}<1.1$.

Figure 7 displays the dependence of Δu_{eff} and $\Delta\omega$ on H for the mixture with $\rho_L=0.8$, $\eta_S=0.028$, and $q=0.3$ in the center of the q2D simulation cell. The values of Δu_{eff}(3D) shown in Fig. 7(a) were calculated using Eq. (3.12) in [9] with the same η_S. The result in 3D is significantly smaller than the q2D depletion interactions when $H=1.1$, with a 3D/q2D ratio of about 1/10 when $r_{12}=1$. We note that this value at $r_{12}=1$ displays a smooth transition as the system confinement changes from q2D to 3D, notwithstanding the oscillatory behavior for larger r_{12}. In Fig. 7(b) we display $\Delta\omega$ for the same q2D system. There is a marked decrease in the amplitude of the oscillations of $\Delta\omega$ as H increases.

Figure 8 shows the dependence of and on H, at the layers of the walls, for the same mixture as discussed with respect to Fig. 7. As before, the values of Δu_{eff}(3D) shown were calculated using Eq. (3.12) of Ref. [9] with the same η_S.

Finally, Fig. 9(a) shows the dependence of Δu_{eff} and $\Delta\omega$ on ρ_L for the case $H=1.1$, $q=0.3$, and $\eta_S=0.028$. The calculated Δu_{eff}(3D) is also shown. Since Δu_{eff}(3D) is not dependent on ρ_L in 3D it serves equally well for comparison with all three different simulation results. Unlike 3D systems, Δu_{eff} in a q2D system is slightly sensitive to ρ_L because $N_S/(\textit{actual free volume})$ increases as the system becomes more densely populated with large spheres. This variation is negligible in 3D when the density of large spheres is low; but in the more compact q2D system it results in a distinguish-

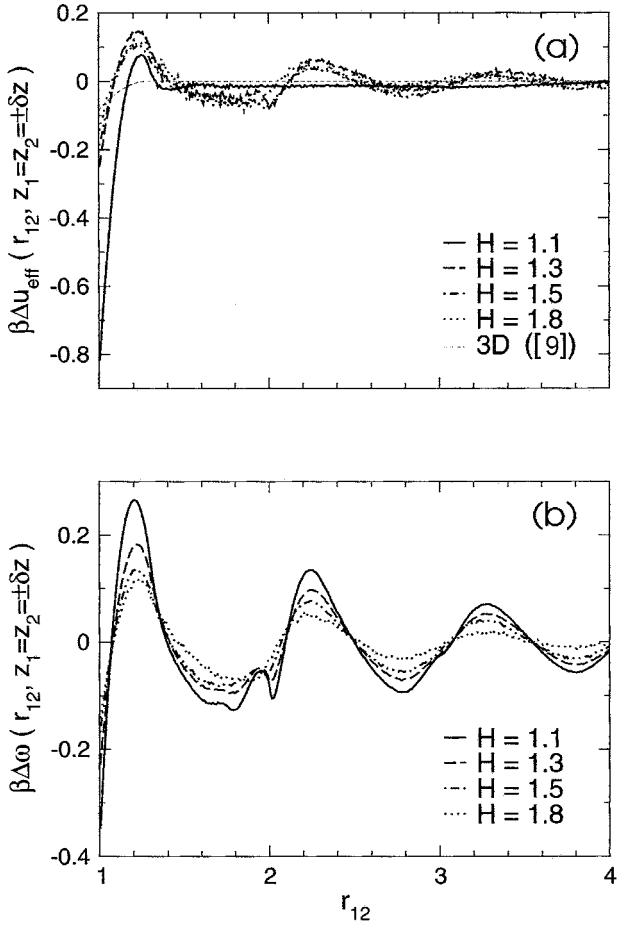

FIG. 7. (a) $\Delta\omega$ and (b) Δu_{eff} in the center of the q2D cell as a function of H when ρ_L=0.8, q=0.3, and η_S=0.028. The 3D effective pair potential shown was calculated using Eq. (3.12) of Ref. [9].

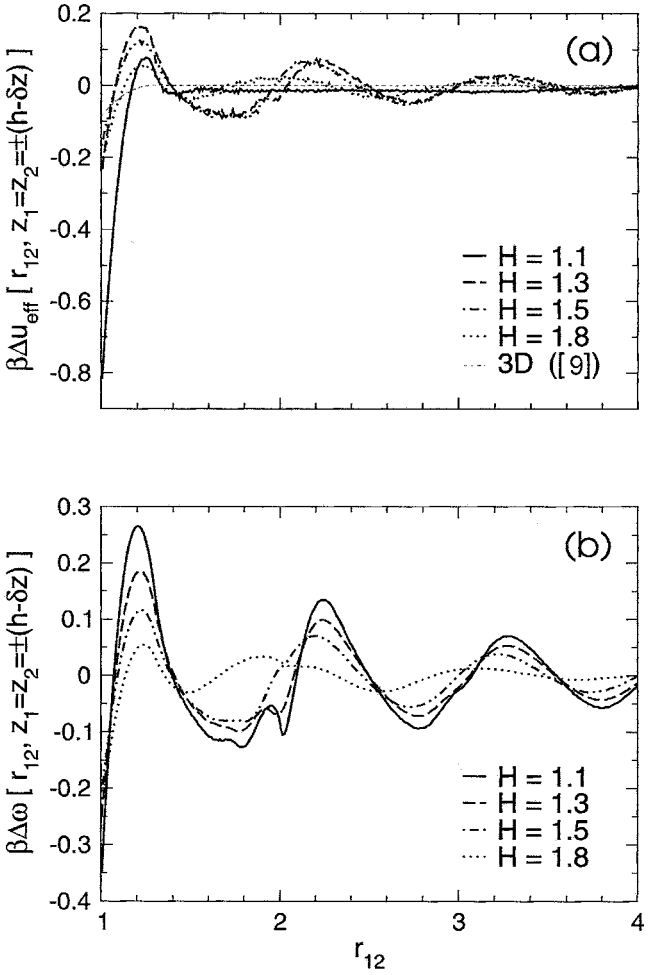

FIG. 8. (a) $\Delta\omega$ and (b) Δu_{eff} at the wall of the q2D cell as a function of H when ρ_L=0.8, q=0.3, and η_S=0.028. The 3D effective pair potential shown was calculated using Eq. (3.12) of Ref. [9].

able enhancement in depletion interaction. Fig. 9(b) shows that the amplitudes of the oscillations of $\Delta\omega$ increase as ρ_L increases; there are also shifts to smaller separation of the secondary and tertiary peaks of $\Delta\omega$ as ρ_L increases.

IV. DISCUSSION

Castaneda-Priego, Rodriguez-Lopez, and Mendez-Alcarez (PLA) [12] have reported the results of studies of the depletion interaction in 2D hard disk mixtures. They define the depletion interaction in a fashion analogous with Eq. (3.2), i.e., as the effective interaction between the large disks, but they focus attention on the limit in which the pair of large disks is infinitely dilute in the fluid of small disks. A comparison of their results and ours is hindered by the difficulty of reconciling the definitions of the small particle packing fraction in the two studies. In the PLA study the small disk packing fraction is defined by coverage of the plane, whereas in our study the small sphere packing fraction is defined in terms of the volume occupied. If we imagine that the centers of all of the small spheres in the q2D system lie in the midplane between the confining walls we can correlate the PLA area fraction with our volume packing fraction by considering the ratio $\phi_S^{\text{PLA}}/\eta_S=(\pi N_S\sigma_S^2/4A)/(N_S\sigma_S^3/6AH)$. Considering only qualitative features of the 2D and q2D simulation results, the most apt comparison between the PLA results and those reported in this paper is for the data set shown in Fig. 6(a) with H=1.1, ρ_L=0.8, and q=0.3. In that case, noting that the small spheres have diameter 0.3, the cell wall separation corresponds to $3.67\sigma_S$, and $\phi_S^{\text{PLA}}/\eta_S$=17.3, so the q2D mixture with η_S=0.028 is to be compared with the 2D mixture with ϕ_S^{PLA}=0.48. Comparing the data in Fig. 3 of Ref. [12] with the data in Fig. 6(a) of this paper reveals that the magnitude of the effective potential in the 2D binary hard disk mixture is about one order of magnitude larger and it has more prominent oscillations as a function of r_{12} than does the effective potential in the q2D binary hard sphere mixture. Clearly, the effect of deviations from 2D geometry must be considered in any analysis of experimental data since only q2D geometries can be realized in the real world.

By collecting the pair correlation functions and extracting effective pair potentials in different layers, we find nonzero effective pair potentials in bare one-component systems. This potential [Figs. 5(a) and 5(b)] has an attractive ($1.5k_BT$) well and oscillates around zero with period σ_L. The source of the

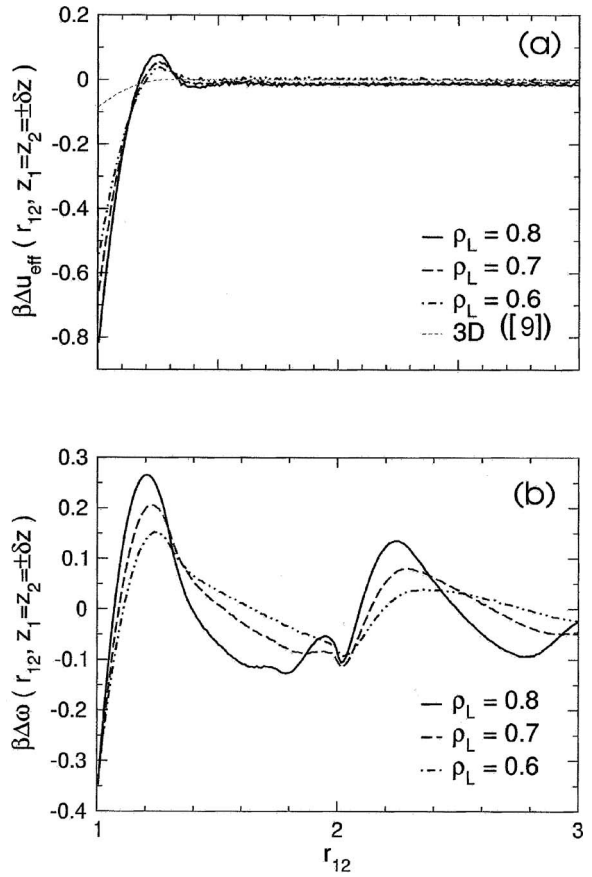

FIG. 9. (a) $\Delta\omega$ and (b) Δu_{eff} as a function of ρ_L when $H=1.1$, $q=0.3$, and $\eta_S=0.028$. The 3D effective pair potential shown was calculated using Eq. (3.12) of [9].

potential is from the structure of the particles in the neighboring layers and is not observed in single-slice systems ($H=1.1$). This potential is purely entropic and depends only on the density and the geometry of the system.

We note that the magnitude of Δu_{eff} under all the conditions considered in this paper is of order a few tenths of k_BT, and that of $\Delta\omega$ typically a factor of two larger. These values are much smaller than inferred from the experimental data of Cui *et al.* [1]. Consequently, we must admit that a hard sphere mixture enclosed between smooth hard plates does not adequately represent the experimental system. We show elsewhere [13] that modifying the model system by inclusion of distributions of the large and small sphere diameters has profound effects on Δu_{eff} but still does not account for the experimental data. We suggest that in the experimental q2D system the influence of the interface between the hydrophobic cell walls and the aqueous colloid suspension on the effective colloid–colloid interaction is more important than generally believed to be the case. Indeed, elsewhere [18] we have shown that a q2D colloid suspension of the same particles as studied by Cui, Lin, and Rice is more confined to the midplane of the cell than expected. The distribution of colloid particle displacements along the z direction was used to infer an effective one body potential. It was speculated that this potential has its origin in the nonwetting of the cell wall by the aqueous colloid suspension. It is not known if a one-body potential of similar origin acts on the small colloid particles in the binary mixture studied by Cui *et al.* Unless that one-body potential constrained the centers of the small spheres to the midplane with sensibly no motion in the z direction, the increase in the depletion interaction will not be large enough to account for the experimental data [13].

ACKNOWLEDGMENTS

The research reported in this paper was supported by a grant from the National Science Foundation CHE-9977841. We have also benefited from the support of the National Science Foundation funded MRSEC Laboratory (under Grant No. DMR-0213745) at The University of Chicago.

[1] B. Cui, B. Lin, D. Frydel, and S. A. Rice, Phys. Rev. E(to be published).
[2] P. D. Kaplan, L. P. Faucheux, and A. J. Lichaber, Phys. Rev. Lett. **73**, 2793 (1994).
[3] R. Dickman, P. Attard, and V Simonian, J. Chem. Phys. **107**, 279 (1994).
[4] B. Gotzelmann and S. Dietrich, Phys. Rev. E **55**, 2993 (1997).
[5] R. Zangi and S. A. Rice, Phys. Rev. E **61**, 660 (2000).
[6] S. Asakura and F. Oosawa, J. Chem. Phys. **22**, 1255 (1954).
[7] A. Vrij, Pure Appl. Chem. **48**, 471 (1976).
[8] T. Biben, P. Bladon, and D Frenkel, J. Phys.: Condens. Matter **8**, 10799 (1996).
[9] B. Gotzelmann, R. Evans, and S. Dietrich, Phys. Rev. E **57**, 6785 (1998).
[10] M. Dijkstra, R. van Roij, and R. Evans, Phys. Rev. E **59**, 5744 (1999).
[11] R. Roth and R. Evans, Phys. Rev. E **62**, 5360 (2000).
[12] R. Castaneda-Priego, A. Rodriguez-Lopez, and J. M. Mendez-Alcaraz, J. Phys.: Condens. Matter **15**, S3393 (2003).
[13] D. Frydel and S. A. Rice, Phys. Rev. E **71**, 041403 (2005).
[14] M. Schmidt and H. Lowen, Phys. Rev. E **55**, 7228 (1997).
[15] P. Attard, J. Chem. Phys. **91**, 3083 (1987).
[16] W. G. McMillan and J. E. Mayer, J. Chem. Phys. **3**, 276 (1945).
[17] N. G. Almarza and E. Lomba, Phys. Rev. E **68**, 011202 (2003).
[18] B. Cui, B. Lin and S. A. Rice, J. Chem. Phys. **116**, 3119 (2002).